Lithos 208–209 (2014) 471–483

Contents lists available at ScienceDirect

Lithos

journal homepage: www.elsevier.com/locate/lithos

Oxygen isotopes in Indian Plate eclogites (Kaghan Valley, Pakistan): Negative $\delta^{18}O$ values from a high latitude protolith reset by Himalayan metamorphism

Hafiz Ur Rehman [a,*], Ryoji Tanaka [b], Patrick J. O'Brien [c], Katsura Kobayashi [b], Tatsuki Tsujimori [b], Eizo Nakamura [b], Hiroshi Yamamoto [a], Tahseenullah Khan [d], Yoshiyuki Kaneko [e]

[a] Graduate School of Science and Engineering, Kagoshima University, Kagoshima, Japan
[b] The Pheasant Memorial Laboratory for Geochemistry and Cosmochemistry, Institute for Study of the Earth's Interior, Okayama University, Misasa, Tottori, Japan
[c] Department of Earth and Environmental Sciences, Potsdam University, Germany
[d] Department of Earth and Environmental Sciences, Bahria University, Islamabad, Pakistan
[e] Department of Education, Meisei University, Hodokubo, Hino-shi, Tokyo, Japan

ARTICLE INFO

Article history:
Received 26 June 2014
Accepted 12 September 2014
Available online 22 September 2014

Keywords:
Himalaya
Kaghan
UHP eclogites
Oxygen isotope compositions
Laser fluorination

ABSTRACT

Oxygen isotope compositions are reported for the first time for the Himalayan metabasites of the Kaghan Valley, Pakistan in this study. The highest metamorphic grades are recorded in the north of the valley, near the India–Asia collision boundary, in the form of high-pressure (HP: Group I) and ultrahigh-pressure (UHP: Group II) eclogites. The rocks show a step-wise decrease in grade from the UHP to HP eclogites and amphibolites. The protoliths of these metabasites were the Permian Panjal Trap basalts (ca. 267 ± 2.4 Ma), which were emplaced along the northern margin of India when it was part of Gondwana. After the break-up of Gondwana, India drifted northward, subducted beneath Asia and underwent UHP metamorphism during the Eocene (ca. 45 ± 1.2 Ma). At the regional scale, amphibolites, Group I and II eclogites yielded $\delta^{18}O$ values of +5.84 and +5.91‰, +1.66 to +4.24‰, and −2.25 to +0.76‰, respectively, relative to VSMOW. On a more local scale, within a single eclogite body, the $\delta^{18}O$ values were the lowest (−2.25 to−1.44‰) in the central, the best preserved (least retrograded) parts, and show a systematic increase outward into more retrograded rocks, reaching up to +0.12‰. These values are significantly lower than the typical mantle values for basalts of +5.7 ± 0.3‰. The unusually low or negative $\delta^{18}O$ values in Group II eclogites potentially resulted from hydrothermal alteration of the protoliths by interactions with meteoric water when the Indian plate was at southern high latitudes (~60°S). The stepwise increase in $\delta^{18}O$ values, among different eclogite bodies in general and at single outcrop-scales in particular, reflects differing degrees of resetting of the oxygen isotope compositions during exhumation-related retrogression.

1. Introduction

Eclogites, generally interpreted as subducted basalts or gabbros, can retain both high and low $\delta^{18}O$ (defined as $[(^{18}O/^{16}O_{sample} \div {}^{18}O/^{16}O_{STD}) - 1]$ in which the standard is Vienna standard mean ocean water; VSMOW), in the mantle over long time spans, i.e., more than one billion years after their subduction (e.g., Eiler, 2001; MacGregor and Manton, 1986; Ongley et al., 1987; Perkins et al., 2006; Zheng et al., 1998). Thus, the oxygen isotope geochemistry of eclogites and related mafic rocks is important for understanding melts and fluids derived from deeply subducted oceanic crust. The $\delta^{18}O$ values of mantle-derived (basalts and gabbros) rocks not altered on the seafloor generally show a narrow range of ca. +5.7 ± 0.3‰ (Hoefs, 2009). If altered, they exhibit a much wider range of ca. 3.6 to +12.7‰ (e.g., Alt et al., 1986; Kawahata et al., 1987). Study of the oxygen isotope compositions of eclogites can help in understanding the nature of the source-rocks (e.g., degrees of alteration on the seafloor prior to subduction) and also the effects of prograde and exhumation-related metamorphism. Most eclogitic rocks have $\delta^{18}O$ values equal to or higher than typical mantle values, reflecting the combined effects of seafloor alteration and subduction zone metamorphism. However, some ultrahigh-pressure (UHP) localities such as the Dabie–Sulu in China (Fu et al., 2013; Yui et al., 1997; Zheng et al., 2003a,b) and Kokchetav in Kazakhstan (Masago et al., 2003) exhibit $\delta^{18}O$ values considerably lower than those typical of the mantle. In this study, we report a third UHP locality (Himalayan eclogites in the Kaghan Valley) at which eclogitic rocks have low, even negative, $\delta^{18}O$ values. Our results for these UHP eclogites, and their retrogressed counterparts (amphibolites), are important for understanding the magmatic and early alteration

* Corresponding author. Tel.: +81 99 285 8147; fax: +81 99 259 4720.
E-mail addresses: hafiz@sci.kagoshima-u.ac.jp (H.U. Rehman), ryoji@misasa.okayama-u.ac.jp (R. Tanaka), obrien@geo.uni-potsdam.de (P.J. O'Brien).

http://dx.doi.org/10.1016/j.lithos.2014.09.007
0024-4937/

history of these rocks and degrees of fluid–rock interaction during subduction-related prograde and retrograde metamorphic processes.

2. Geological setting

The Himalayan metamorphic belt resulted from the collision of Indian and Asian plates sandwiching the Kohistan–Ladakh island Arc (KLA) (Fig. 1). It represents a classic example of a continent–continent collision following the subduction of continental lithosphere to mantle depths (>100 km) where the leading edge of India experienced UHP metamorphism before multi-step exhumation (Kaneko et al., 2003; O'Brien et al., 2001; Rehman et al., 2007; Tahirkheli et al., 1979; Wilke et al., 2010a and references therein). The metamorphic rocks in the Indian plate that are bound to the KLA in the north by the main mantle thrust comprise the amphibolite to eclogite facies series, which belong to the Higher Himalayan Crystalline (HHC), and the greenschist to amphibolite facies series, which are attributed to the Lesser Himalayan Sequence (Chaudhry and Ghazanfar, 1987; Greco et al., 1989).

Protoliths of the Himalayan eclogites and related mafic rocks are generally considered as the Permo-Triassic Panjal Trap continental flood basalts and their feeder dikes of the Gondwana affinity (Honegger et al., 1982; Papritz and Rey, 1989). The age of emplacement of these rocks is well constrained between 253 and 269 Ma based on U–Pb dating of zircon, rutile and titanite (e.g., Parrish et al., 2006; Rehman et al., 2013; Spencer and Gebauer, 1996; Wilke et al., 2010a). However, their source rock characteristics are poorly known. Moreover, after the break-up from Gondwana, the Indian plate drifted northward for several thousand kilometers before colliding with Asia during the Eocene, where a considerable portion of the Indian plate margin was initially subducted beneath Asia (Guillot et al., 2003). Eclogite facies metamorphism in the Kaghan Valley occurred at 45 Ma (U–Pb zircon, rutile and titanite Kaneko et al., 2003; Parrish et al., 2006; Rehman et al., 2013; Wilke et al., 2010a). During exhumation partial to complete amphibolitization of eclogites took place. This stage is dated at around 40 Ma based on ^{40}Ar–^{39}Ar dating of phengite and hornblende (Chamberlain et al., 1991; Wilke et al., 2010a). Oxygen isotope analyses of these UHP eclogites reveal information regarding magmatic source rocks and paleo-environment and fluid–rock interactions during their subduction and exhumation.

3. Sampling strategy and rock description

To understand the source rock characteristics and alteration at the hand-sample scale, we obtained $\delta^{18}O$ values for whole-rock samples (referred as $\delta^{18}O_{wr}$). In addition, to evaluate the effects of metamorphic fluids on these rocks during peak (eclogite facies) and retrograde (amphibolite facies) stages, we obtained $\delta^{18}O$ values for peak eclogite facies minerals and those typical of late-stage retrogression. The $\delta^{18}O$ values of individual minerals are referred as $\delta^{18}O_{min}$. Our study was conducted at both the outcrop scale (single UHP eclogite body of approximately 2 m in diameter) and the regional scale (one block of amphibolitized eclogites and four blocks of eclogites spreading in an area of about 10 km distance). Sample details are given in Table 1 and their locations are shown in Fig. 2. For most of these samples, thermobarometric information, whole rock major and trace element compositions, whole rock and mineral ^{147}Sm–^{143}Nd and ^{176}Lu–^{176}Hf isotopic data, and zircon U–Th–Pb ages have previously been reported (Rehman et al., 2007, 2008, 2012, 2013). Mineral abbreviations used throughout this study are after Whitney and Evans (2010) except symplectites are abbreviated as "Sym".

3.1. Amphibolitized eclogites

Two samples (Ph241 and Ph245) were collected from the heavily amphibolitized eclogite body south of Besal (Fig. 2) where they appear as small lenticular blocks or sheets within felsic/pelitic gneisses and

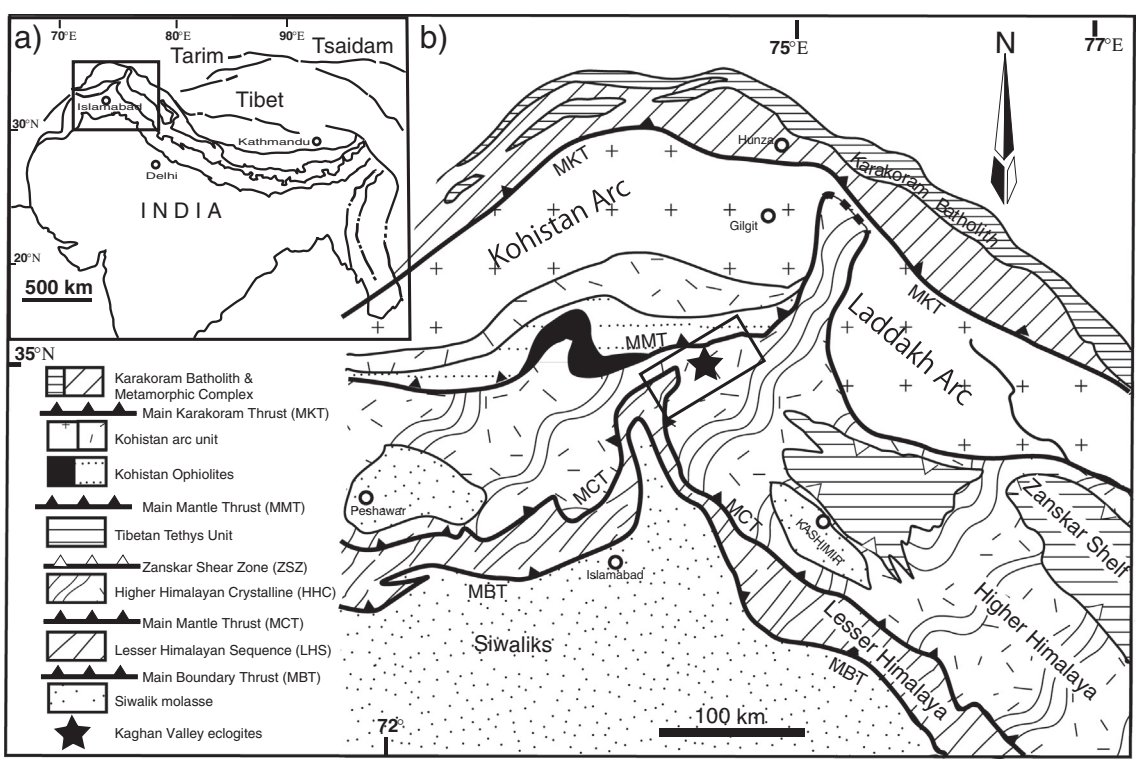

Fig. 1. Regional geological map of the Himalayan range. (a) A general sketch of the Himalayan range. The small rectangle represents the portion enlarged in b. (b) Major tectonic units of the Indian plate, the Kohistan–Ladakh arc and the northern portion of the Asian plate.
Modified after Searle et al., 1999; Kaneko et al., 2003.

Table 1
Oxygen isotope compositions of the selected whole-rock samples from the Himalayan metabasites.

Unit	Location	Latitude (N°)/ longitude (E°)	Sample No	Rock type	Mineral assemblage[a]	$\delta^{18}O$ (‰)	$\delta^{17}O$ (‰)	$\Delta^{17}O_{TSFL}$ (‰)[b]
Regional distribution								
HHC	South of Besal	35° 01′ 32.55″N 73°	Ph241	Amphibolite	**Amp** + **Grt** + Qz + Bt + Zo + Chl ± Sym ± Rt ± Ttn ± Ap ± Opq	5.84	3.00	0.002
		56′ 24.17″E	Ph245	*ditto*	**Amp** + **Grt** + **Qz** + Bt + Zo + Chl ± Sym ± Rt ± Ttn ± Ap ± Opq	5.91	2.97	−0.072
	East of Lulusar	35° 06′ 25.54″N 73°	Ph408	HP eclogite	**Grt** + **Omp** + Amp + Zo + Qtz + Sym + Ph + Bt ± Rt ± Ttn ± Zrn ± Ap ± Opq	3.45	1.78	0.037
		58′ 36.88″E	Ph409	*ditto*	**Grt** + **Omp** + Amp + Zo + Qtz + Sym + Ph + Bt ± Rt ± Ttn ± Zrn ± Ap ± Opq	4.09	2.13	0.050
			Ph410	*ditto*	**Grt** + **Omp** + Qtz + Amp + Ph + Zo ± Rt ± Ttn ± Ap ± Zrn ± Opq	4.24	2.17	0.008
	Northwest of Lulusar	35° 5′ 32.71″N 73°	Ph378	Amphibolitized eclogite	**Amp** + **Grt** + **Sym** + **Bt** ± Cpx ± Qtz ± Rt ± Ttn ± Ap ± Zrn ± Opq	2.59	1.31	0.017
		53′ 38.28″E	Ph380	HP eclogite	**Grt** + **Omp** + Sym + Amp + Qtz + Rt + Ttn ± Ap ± Zrn ± Opq	1.80	0.90	0.017
			Ph381	*ditto*	**Grt** + **Sym** + **Amp** + Omp + Qtz + Ap ± Rt ± Bt ± Ttn ± Ap ± Zrn ± Opq	1.66	0.83	0.027
	North of Lulusar	35° 05′ 44.71″N 73°	Ph449	UHP eclogite	**Grt** + **Omp** + Qtz + Sym + Amp + Ph + Zo ± Rt ± Ttn ± Ap ± Zrn ± Opq	0.23	0.08	0.032
		55′ 31.65″E	Ph450	*ditto*	**Grt** + **Sym** + **Amp** + Omp + Qtz + Ph + Zo ± Rt ± Ttn ± Ap ± Zrn ± Opq	0.71	0.32	0.010
			Ph456	*ditto*	**Grt** + **Omp** + Qtz + Amp + Sym + Ph + Zo ± Rt ± Ttn ± Ap ± Zrn ± Opq	0.76	0.31	−0.021
	West of Gittidas	35° 06′ 56.88″N 73°	Ph422	UHP eclogite	**Grt** + **Omp** + **Zo** + Sym + Amp + Ph + Qtz ± Rt ± Ttn ± Ap ± Zrn ± Opq	−2.05	−1.08	0.068
		58′ 06.91″E	Ph423	*ditto*	**Grt** + **Omp** + **Zo** + **Ph** + Sym + Amp + Qtz / Coe ± Rt ± Ttn ± Ap ± Zrn ± Opq	−2.14	−1.16	0.042
			Ph425	*ditto*	**Grt** + **Omp** + **Zo** + Sym + Amp + Ph + Qtz / Coe + Rt + Ttn ± Ap ± Zrn ± Opq	−2.07	−1.20	−0.036
			Ph426	Amphibolitized eclogite	**Grt** + **Amp** + **Sym** + Omp + Qtz ± Rt ± Ttn ± Ap ± Zrn ± Opq	0.94	0.43	0.001
			Ph427	UHP felsic gneiss	**Pl** + **Qtz** + Bt ± Zo ± Grt ± Rt ± Ttn ± Ap ± Aln ± Zrn ± Opq	4.58	2.39	0.048
			Ph428	*ditto*	**Pl** + **Qtz** + Bt ± Zo ± Grt ± Rt ± Ttn ± Ap ± Aln ± Zrn ± Opq	3.03	1.51	−0.010
Local distribution (within a single UHP eclogite unit)								
HHC	West of Gittidas		Ph514	UHP eclogite	**Grt** + **Omp** + Sym + Amp + Zo + Ph + Qtz / Coe + Rt + Ttn ± Ap ± Zrn ± Opq	−2.09	−1.14	0.027
			Ph513	*ditto*	**Grt** + **Omp** + Sym + Amp + Ph + Qtz/Coe + Zo + Rt + Ttn ± Ap ± Zrn ± Opq	−2.25	−1.21	0.040
			Ph506	*ditto*	**Grt** + **Omp** + **Zo** + Sym + Ph + Qtz / Coe + Amp ± Rt ± Ttn ± Ap ± Zrn ± Opq	−1.44	−0.79	0.039
			Ph507	*ditto*	**Grt** + **Omp** + Zo + Sym + Amp + Ph + Qtz / Coe ± Rt ± Ttn ± Ap ± Zrn ± Opq	−2.25	−1.22	0.037
			Ph508	Amphibolitized eclogite	**Grt** + **Sym** + **Amp** + Omp + Ph + Zo + Qtz ± Rt ± Ttn ± Ap ± Zrn ± Opq	−0.11	−0.12	0.010
			Ph509	Amphibolite	**Amp** + **Grt** + **Sym** + **Zo** + Qtz ± Rt ± Ttn ± Ap ± Zrn ± Opq	0.12	0.04	0.042
			Ph510	UHP felsic gneiss	**Pl** + **Qtz** + Ph ± Amp ± Bt ± Zo ± Rt ± Ilm ± Ap ± Zrn ± Opq	4.01	2.05	0.010
			Ph511	*ditto*	**Pl** + **Qtz** + Ph ± Amp ± Bt ± Zo ± Rt ± Ilm ± Ap ± Zrn ± Opq	4.08	2.10	0.023

[a] Minerals shown in "bold type font" are in abundance.
[b] $\Delta^{17}O_{TSFL} = \ln(\delta^{17}O + 0.07 \times 10^{-3} + 1) - 0.527\ln(\delta^{18}O + 1)$ defined by Tanaka and Nakamura (2013).

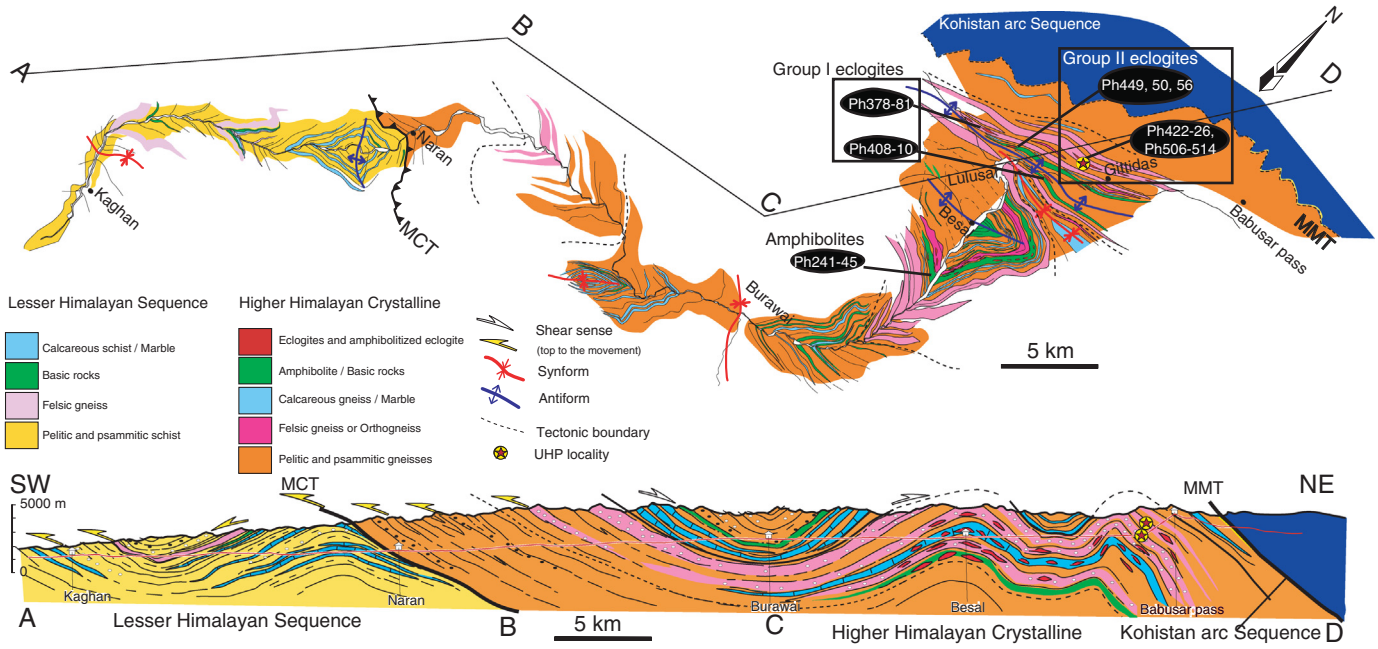

Fig. 2. Geological map and sample location of the Himalayan metamorphic belt along the Kaghan Valley transect. Modified after Kaneko et al., 2003; Rehman et al., 2007.

metacarbonates. Petrographically, these rocks are composed mainly of Amp and Grt with less Qz, Bt, Zo, Sym, Chl, Opq, and accessory Rt, Ttn and Ap. Amphibole appears in two generations, as coarse-grained porphyroblasts and in fine-grained albite–amphibole–quartz symplectites "Sym" (Fig. 3a). Most garnets have Amp and Bt along their rims. The symplectites, formed after omphacite, indicate that the rocks were once eclogites. Peak pressure–temperature (P–T) conditions for the amphibolites were estimated at 0.8 ± 0.1 GPa and 673 ± 55 °C (Rehman et al., 2007).

3.2. Eclogites

The eclogites and their slightly retrograde equivalents occur as thin sheets to massive bodies that are a few meters to a few tens of meters thick and surrounded by felsic gneisses and metacarbonates. The samples studied here are from four main locations (Fig. 2): east of Lulusar (Ph408–410); northwest of Lulusar (Ph378, Ph380 and Ph381); north of Lulusar (Ph449, Ph450 and Ph456) and west of Gittidas (Ph422, Ph423, Ph425 and Ph426). The former two locations are HP eclogites (termed as Group I) whereas the latter two are UHP (Group II) eclogites. All of these eclogites contain Grt, Omp, Amp, Qz, Rt, Ttn, Ap and Zrn. Apart from Ph380 and Ph381 all contain Zo and Ph. The degree of retrogression is reflected in the amount of Sym (high in amphibolitized eclogite of Ph378 and low in UHP eclogite of Ph425), Ttn replacing Rt and secondary Pl in Sym. Coesite relics, indicating UHP conditions, were previously documented for Group II eclogites (Rehman et al., 2007). The eclogites show considerable ranges in their concentrations of SiO_2 (42–50 wt.%), Al_2O_3 (11–16 wt.%), TiO_2 (2–5 wt.%), total FeO (13–19 wt.%) and Na_2O (1.5–3.1 wt.%; Rehman et al., 2008), even within a single boudin in which the variations are believed to reflect primary magmatic signatures in the protoliths.

Relatively "fresh" eclogites of the Group I (Ph410; Fig. 3b) exhibit a granoblastic texture of Grt and Omp with secondary Amp and only minor replacement by Bt and Sym at the Grt-Omp contacts. Similarly, sample Ph380 (collected from different block) is medium to coarse-grained and contains abundant rounded to subrounded Grt porphyroblasts, anhedral Omp rimmed by symplectitic Amp and abundant Rt and Ttn (Fig. 3c). In sample Ph378, collected from the amphibolitized margin of the same eclogite body, Omp is completely replaced by Sym (Fig. 3d). In contrast, samples Ph423 and Ph425 (Group II) contain fresh Omp and Grt with only minor Sym (Fig. 3e). Previous studies of the Group II eclogites (e.g., Kaneko et al., 2003; O'Brien et al., 2001; Rehman et al., 2007; Wilke et al., 2010a,b) have indicated minimum peak P–T conditions of 2.7 GPa (using Grt–Cpx–Ph geobarometry of Waters and Martin, 1993) and 768 ± 46 °C (based on the Fe–Mg exchange in Grt-Cpx; Powell, 1985, and the Grt–Ph thermometry of Green and Helman, 1982) corresponding to conditions at upper-mantle depths during deep continental subduction.

3.3. Felsic gneisses

Two felsic gneisses (Ph427 and Ph428) in contact with the UHP eclogite were sampled west of Gittidas. These samples contained abundant Qz with PL, Zo, Aln, Bt, Ph, Grt, Ttn and Zrn. Inclusions of coesite in Zrn (Kaneko et al., 2003) confirm the UHP conditions experienced by these rocks.

3.4. Detailed sampling of a single m-scale UHP eclogite body and surrounding rocks

To determine how fluid-driven retrograde metasomatism affects oxygen isotope variability at the outcrop scale, samples were collected west of Gittidas (Fig. 2) from a 2-m single UHP body and its surrounding felsic gneisses. In this body, zoning was observed outward from the core of fresh eclogite to heavily retrogressed eclogite to amphibolite in contact with felsic gneisses, and samples were collected considering the core of the body as the least modified by retrograde fluid–rock interactions.

4. Analytical procedure

Sample preparation and oxygen isotope analyses were carried out at the Okayama University, Misasa, Japan. Whole-rock powders were prepared from 2 mm-sized chips crushed in a steel jaw crusher. Fresh pieces of the crushed rock were handpicked and washed with deionized water in an ultrasonic bath for 30 min, dried at 110 °C overnight, and pulverized in a silicon nitride mortar. Mineral fractions were separated from the sieved fraction (200 to 250 μm size), cleaned in an ultrasonic

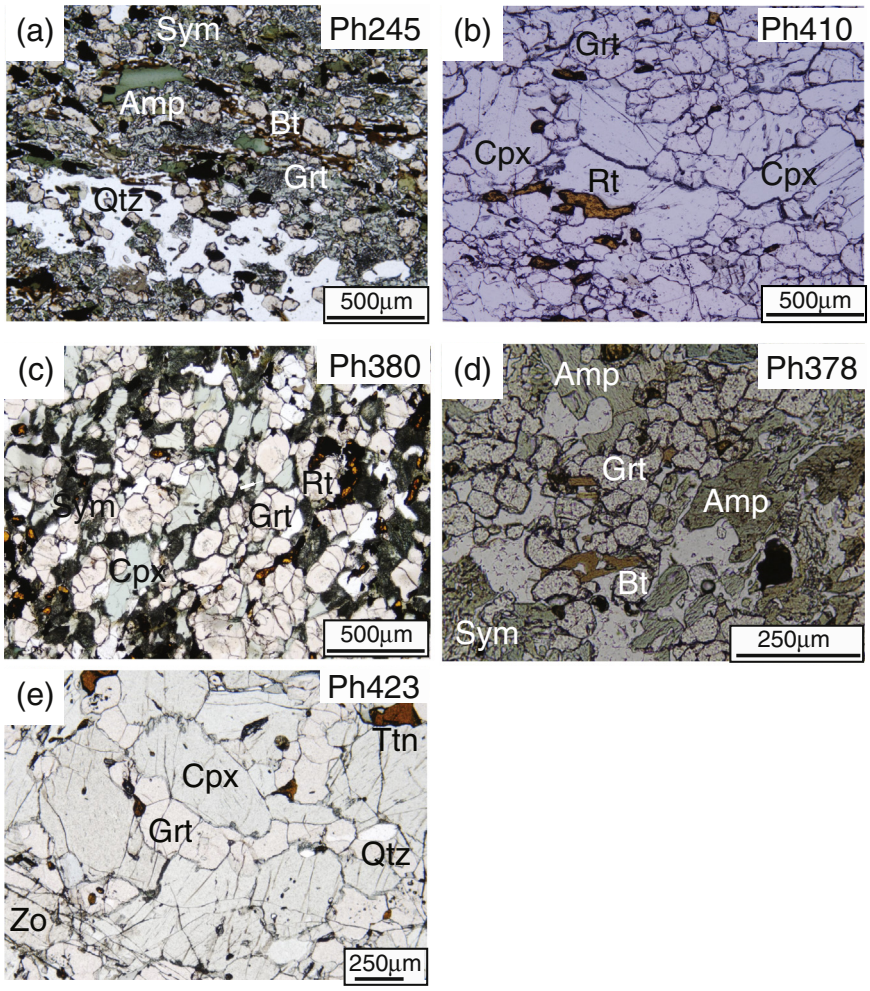

Fig. 3. Photomicrographs of (a) amphibolitized eclogite (Ph245) displaying two generations of amphibole: (1) medium to coarse-grained well-developed porphyroblasts and (2) fine-grained symplectites after the replacement of Omp. (b) Fresh eclogite (Ph410) displaying a granoblastic texture. Most of the Grt and Omp grains are fresh. Rt occurs as inclusions in Grt and Omp and as growths along the grain boundaries. (c) HP eclogite (Ph380) exhibiting rounded Grt porphyroblasts with elongated Omp grains. Most of the Omp grains have darker outlines along their rims (symplectites). (d) Highly retrogressed eclogite (Ph378) in which Omp has been completely replaced by porphyroblastic and symplectitic Amp and Bt. (e) UHP grade fresh eclogite (Ph423) having well-developed porphyroblasts of Grt and Omp with almost no retrogressive phases.

bath for 30 min, and dried at 90 °C for a minimum of 24 h. Magnetic and non-magnetic minerals were separated with a Franz magnetic separator and finally handpicked under a binocular microscope to avoid grains with discernable mineral inclusions or alterations. Next, the separated minerals were allowed to react with 1 M HCl for 2–4 h to remove surface contamination, washed with deionized water, and dried overnight at 110 °C.

Oxygen in the sample was extracted by laser fluorination method, and the $^{17}O/^{16}O$ and $^{18}O/^{16}O$ were measured on the dual inlet gas source mass spectrometers using VG SIRA12 and Thermo MAT253. Details regarding the mass spectrometry performed by VG SIRA12 and Thermo MAT253 were reported by Kusakabe et al. (2004) and Tanaka and Nakamura (2013), respectively. The $^{17}O/^{16}O$ and $^{18}O/^{16}O$ of the unknown samples were expressed by the deviation of the isotopic ratios relative to VSMOW as $\delta^{17}O$ and $\delta^{18}O$, respectively. All the data are plotted on the terrestrial silicate fractionation line defined by Tanaka and Nakamura (2013) (definition is shown in footnote of Table 1). The $\delta^{17}O$ and $\delta^{18}O$ values of the reference samples that were analyzed by VG SIRA12 were +3.05 ± 0.08‰ and +5.99 ± 0.05‰ (n = 37, 1SD) for MSG-1 (Grt: an in house standard) and +2.89 ± 0.04‰ and +5.74 ± 0.08‰ (n = 14, 1SD) for UWG-2 (Grt standard), respectively. The values obtained from Thermo MAT253 were +4.90 ± 0.05‰ and 9.43 ± 0.08‰ (n = 20, 1SD) for NBS-28 (Qz standard) and +3.08 ± 0.05‰ and 6.00 ± 0.08‰ (n = 20, 1SD) for MSG-1, respectively. To avoid cross-contamination and partial fluorination of the plagioclase and whole rock powders (which are easily fluorinated at room temperature), only one batch of these samples was installed in a reaction chamber with the garnet standard (MSG-1) at a time, then plagioclase or whole rock powder was first fluorinated in each reaction chamber (see the detail of fluorination system in Tanaka and Nakamura, 2013).

5. Results

The $\delta^{18}O_{wr}$ values for all samples are given in Table 1 and mineral modal abundances for the representative samples that were analyzed are shown in Fig. 4. The $\delta^{18}O$ values of the minerals ($\delta^{18}O_{min}$) separated from each rock are presented in Table 2, and the $\delta^{18}O$ data on regional and outcrop scales are summarized in Figs. 5 and 6, respectively.

For all whole-rock samples combined, the $\delta^{18}O_{wr}$ values vary from −2.25‰ to +5.91‰. Analysis of the two heavily amphibolitized eclogite samples (Ph241 and Ph245) yielded the highest $\delta^{18}O_{wr}$ values of +5.84 and +5.91‰, respectively. The $\delta^{18}O_{min}$ data for these two samples show a narrow range scattered around the whole-rock data (see Table 2 for details). The $\delta^{18}O_{wr}$ values of the HP eclogites (Group I) range from +1.66 to +4.24‰. Eclogites from east of Lulusar (Ph408–410) had higher (+3.45 to +4.24‰) values than those from northwest of Lulusar (Ph378–381: +1.66 to +2.59‰). The $\delta^{18}O_{min}$

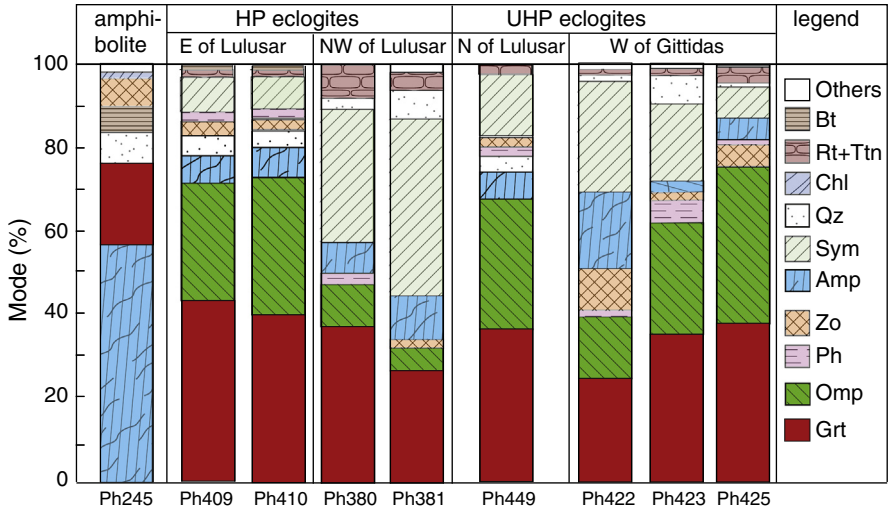

Fig. 4. Modal abundances (vol. %) of major mineral assemblages in representative samples from the amphibolites and eclogites. Modal abundance was determined using the point-counting technique on thin sections. The abundance of each mineral was based on the calculated average of 2500 points for each thin section.

data for these eclogites are also scattered in identical manner around the $\delta^{18}O_{wr}$ values as shown in Table 2. The slightly higher $\delta^{18}O_{wr}$ values in eclogites east of Lulusar (despite their less retrogressed nature) compared with the same group of eclogites northwest of Lulusar might indicate heterogeneous alteration of the protoliths.

The UHP eclogites (Group II) from two sampling locations have low but different $\delta^{18}O$. Samples from the north of Lulusar (Ph449, Ph450 and Ph456) have $\delta^{18}O_{wr}$ values of +0.23 to +0.76‰ whereas eclogite sampled from west of Gittidas (Ph422, Ph423, Ph425, Ph506, Ph507, Ph513, and Ph514) had $\delta^{18}O_{wr}$ values of −2.25 to −1.44‰. The $\delta^{18}O_{min}$ values of these eclogites, like the whole-rock data, are also lower than the values obtained for other samples studied (Table 2). However, the amphibolitized eclogite (Ph426) have values higher than those of eclogites from the same locality. It is important to note that felsic gneisses of UHP grade from the location west of Gittidas (Ph427, Ph428, Ph510, and Ph511) also yielded $\delta^{18}O_{wr}$ values between +4.58 and +3.03‰ that are lower than the values normally reported for metasedimentary rocks (Hoefs, 2009; Kolodny and Epstein, 1976).

For the single UHP eclogite body west of Gittidas, $\delta^{18}O_{wr}$ values of −2.25 to −1.44‰ were obtained for the fresh eclogites (Ph506–507 and Ph513–514) and $\delta^{18}O_{wr}$ values of −0.11‰ and +0.12‰ were obtained for the amphibolitized eclogite (Ph508) and amphibolite (Ph409), respectively. In contrast, the felsic gneisses (Ph510 and Ph511) have $\delta^{18}O$ of +4.01 and +4.08‰, respectively. These rocks show progressive increase in $\delta^{18}O_{wr}$ outward from the center of the body (Fig. 6).

The two following distinct trends were observed in the analyzed samples: (1) a step-wise increase in the $\delta^{18}O_{wr}$ values from UHP eclogites to HP eclogites to amphibolites (Figs. 5) and (2) progressive increase in $\delta^{18}O_{wr}$ values from the eclogites to the amphibolites at the scale of the individual outcrop (Fig. 6).

The expected sequence of ^{18}O enrichment in typical rock-forming minerals, at thermodynamic equilibrium is: Qz > Ph > Omp > Zo > Hbl > Chl > Grt > Ttn > Rt (Hoefs, 2009; Lacroix and Vennemann, 2013; Zheng et al., 2003c). For the eclogites, the sequence of ^{18}O enrichment in minerals followed this normal enrichment pattern (as shown above). However, ^{18}O enrichment in Amp (mineral related to post-peak pressure metamorphic conditions) is sometimes greater than in Omp (Ph380, Ph410, Ph423, and Ph425), similar to that in Omp (Ph422), or smaller than that in the Grt (Ph381; see Table 2). For the amphibolite samples Ph241 and Ph245, a normal enrichment pattern of ^{18}O was observed. It is important to note that a positive trend was also obtained when the $\delta^{18}O$ values of constituent minerals were plotted against those of Qz (Fig. 7). The trend in $\delta^{18}O_{min}$ values is similar to that observed for whole-rock $\delta^{18}O$. In all the analyzed samples, $\delta^{18}O$ values of amphibole (secondary mineral) shift toward more positive side (Fig. 7).

6. Oxygen isotope thermometry

The temperature dependence of oxygen isotope fractionation between Qz and other mineral pairs (e.g., Grt, Omp, Zo, Ph, Amp, Ttn, and Rt) has been presented by several authors based on theoretical calculations, experimental measurements and empirical estimates (e.g., Chacko et al., 1996; Zheng, 1999; Zheng et al., 2003c). The Zheng (1999) calibrations are consistent with experimental and empirical calibrations and yield reasonable temperatures for mineral pairs when the minerals are at equilibrium.

In the amphibolite samples, fractionation of Qz with Zo, Amp, and Grt yields temperatures of 584, 641 to 679 and 632 to 707 °C, respectively (Table 2). The eclogite samples show an even greater temperature range (Fig. 8). For the preserved eclogite facies minerals, Ph, Omp and Grt fractionation with Qz, yielded minimum and maximum temperatures of 542 and 668 °C, 495 and 621 °C, and 569 and 668 °C, respectively. Minerals that represented post-eclogite-peak retrogression (e.g., Amp, Zo and Ttn) yielded both relatively high (Qz–Amp = 572–699 °C) and low temperatures (Qz–Zo = 516–523 °C, and Ttn = 427–448 °C).

On an isotherm diagram of the oxygen isotope fractionations the Qz–Grt and Qz–Amp in amphibolites (Ph241 and Ph245) plot on the 700 and 650 °C isotherms, respectively, suggest equilibrium among these minerals at those temperatures (Fig. 8a). In contrast, Zo (plotting away from the same isotherm) was likely not in equilibrium with Grt and Amp. In Group I eclogites (east of Lulusar), the Qz–Grt and Qz–Omp in sample Ph408 plot near the 600 °C isotherm but the Qz–Amp plots farther away from that isotherm. In sample Ph410, the Qz–Grt and Qz–Amp plot near the 600 °C isotherm. However, the Qz–Omp pair plots farther away on a lower temperature isotherm (Fig. 8b). Regarding the eclogites from northwest of Lulusar, the Qz and other minerals (Fig. 8c) do not plot on the same temperature isotherms, suggesting isotopic disequilibrium. For the UHP eclogites, the Grt, Amp and Ph presented identical results when the Qz–minerals data were plotted on the isothermal diagram, but the Qz–Omp pair did not (Fig. 8d and e). In general, the calculated temperatures for most of the Qz–mineral pairs in the eclogites and amphibolites show large scatter indicating that the calculated temperatures are not geologically meaningful.

Table 2
The $\delta^{17}O$ and $\delta^{18}O$ values from minerals, the fractionation factors between quartz and other mineral phases, and the calculated temperatures.

Unit	Lithology	Sample no.	Mineral[a]	Number of analyses		O_2 yield (%)	$\delta^{18}O$ (‰)	$\delta^{17}O$ (‰)	$\Delta^{17}O_{TSFL}$ (‰)	$\delta^{18}O_{qz-a}$ (‰)[b]	Temp. (°C)[c]
				SIRA12	MAT253						
S of Besal	Amphibolites	Ph241	Qz	0	2	98	8.66	4.47	−0.009	–	
			Zo	0	2	97	5.50	2.81	−0.011	3.16	584
			Amp	0	2	100	5.46	2.81	0.006	3.20	679
			Grt	0	2	99	5.21	2.66	−0.011	3.45	707
		Ph245	Qz	0	2	99	8.77	4.55	0.002	–	
			Amp	0	2	100	5.30	2.70	−0.020	3.47	641
			Grt	0	2	100	4.73	2.42	−0.005	4.04	632
E of Lulusar	HP eclogites	Ph408	Qz	0	2	100	6.56	3.41	0.026	–	
			Omp	0	2	98	3.37	1.68	−0.023	3.20	575
			Amp	0	2	94	2.82	1.41	−0.008	3.75	607
			Grt	0	2	100	2.54	1.26	−0.003	4.03	634
		Ph410	Qz	0	2	101	7.71	4.01	0.025	–	
			Omp	0	2	103	4.24	2.16	−0.003	3.47	541
			Amp*	0	2	102	4.65	2.39	0.011	3.07	699
			Grt	0	2	99	3.54	1.79	−0.002	4.17	618
			Ttn	0	2	101	0.10	−0.04	−0.025	7.61	427
			Rt	0	1	101	−0.38	−0.31	−0.042	8.09	460
NW of Lulusar	HP eclogites	Ph380	Qz	0	3	99	5.10	2.63	0.018	–	
			Omp	0	2	103	1.99	0.97	−0.013	3.11	587
			Amp*	2	0	103	2.03	0.93	−0.065	3.07	699
			Grt	2	0	93	1.36	0.70	0.054	3.73	668
			Ttn	0	1	97	−2.22	−1.22	0.016	7.32	441
		Ph381	Qz	0	2	99	5.37	2.77	0.012	–	
			Omp	2	0	96	1.92	0.91	−0.034	3.44	544
			Amp*	2	0	90	1.31	0.67	0.053	4.06	572
			Grt	3	2	97	1.54	0.77	0.027	3.83	657
N of Lulusar	UHP eclogites	Ph449	Qz	0	2	100	3.07	1.57	0.020	–	
			Omp	0	3	100	−0.03	−0.07	0.018	3.11	587
			Grt	0	2	98	−0.91	−0.53	0.016	3.98	639
			Rt	0	2	103	−4.30	−2.34	0.001	7.37	495
		Ph456	Qz	0	1	96	4.63	2.33	−0.044	–	
			Omp	0	2	103	0.73	0.35	0.032	3.90	495
			Amp	0	2	100	0.40	0.15	0.006	4.23	555
			Grt	0	2	101	0.20	0.03	−0.006	4.43	591
			Rt	0	2	93	−3.34	−1.83	0.005	7.97	466
W of Gittidas	UHP eclogites	Ph422	Qz	0	3	100	1.11	0.55	0.034	–	
			Ph	2	0	92	−1.43	−0.79	0.041	2.54	608
			Omp	2	0	99	−2.37	−1.32	−0.002	3.48	540
			Zo	2	0	93	−2.55	−1.43	−0.013	3.65	524
			Amp*	2	0	95	−2.37	−1.31	0.015	3.48	640
			Grt	3	1	97	−2.75	−1.50	0.018	3.86	653
			Rt	0	2	98	−6.42	−3.47	−0.006	7.53	487
		Ph423	Qz	0	2	100	1.28	0.63	0.023	–	
			Ph	2	0	94	−1.69	−0.96	0.000	2.96	542
			Omp	2	0	100	−2.17	−1.18	0.030	3.45	544
			Zo	2	0	100	−2.45	−1.35	0.013	3.73	516
			Amp*	2	0	92	−1.98	−1.06	0.052	3.26	670
			Grt	4	0	95	−2.80	−1.55	0.000	4.08	628
			Ttn	0	2	97	−5.90	−3.20	−0.013	7.18	448
			Rt	0	2	96	−6.35	−3.42	−0.002	7.63	482
		Ph425	Qz	0	2	100	1.14	0.55	0.023	–	
			Ph	2	0	97	−1.09	−0.70	−0.058	2.23	668
			Omp	2	0	103	−2.15	−1.26	−0.056	3.29	563
			Zo	2	0	97	−2.52	−1.43	−0.025	3.66	523
			Amp*	2	0	96	−2.00	−1.10	0.019	3.13	689
			Grt	4	0	97	−2.80	−1.57	−0.026	3.94	644
			Rt	0	2	102	−6.55	−3.52	0.005	7.69	479
		Ph426	Qz	0	3	100	4.13	2.13	0.020	–	
			Omp	0	2	100	1.26	0.59	−0.003	2.88	621
			Grt	0	2	99	−0.54	−0.32	0.030	4.67	569
	UHP felsic gneisses	Ph427	Qz	0	2	96	3.61	1.85	0.018	–	
			Bi	0	2	96	0.52	0.20	−0.008	3.09	
			Zo	0	2	103	0.79	0.34	−0.004	2.82	634
			Pl	0	2	98	4.37	2.21	−0.017	−0.76	
		Ph428	Qz	0	3	98	2.89	1.48	0.024	–	
			Pl	0	2	100	2.51	1.27	0.016	0.39	
			Ph	0	2	101	1.60	0.77	−0.001	1.29	962
			Bi	0	2	93	0.16	0.03	0.009	2.73	
			Ilm	0	1	101	−5.96	−3.20	0.018	8.85	

[a] Amp marked with an asterisk have an abnormal sequence of $\delta^{18}O$ enrichment.
[b] The $\delta^{18}O$ value of quartz minus that of the mineral in the same sample.
[c] Temperature values were calculated according to Zheng et al. (2003c).

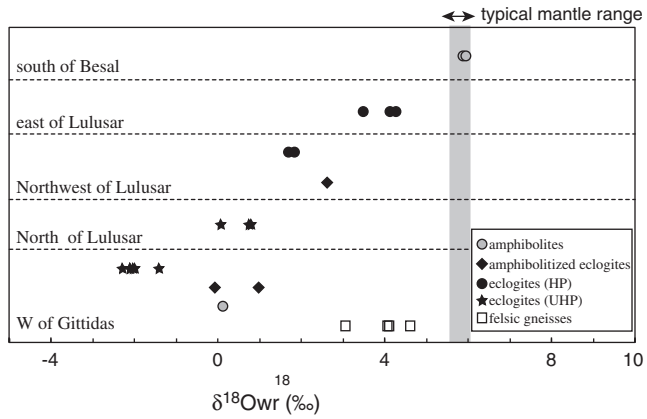

Fig. 5. Plot of $\delta^{18}O_{wr}$ values for the analyzed samples. The local scale (single eclogite body) and regional scale positive trends in the $\delta^{18}O_{wr}$ values can be seen. Analytical errors for the whole-rock samples are less than the symbol size.

7. Discussion

For basalts, the $\delta^{18}O_{wr}$ values of +5.7 ± 0.3‰ (Hoefs, 2009) represent the unaltered mantle source, and most mantle-derived rocks have $\delta^{18}O$ values in the range of +3.6 to 8.7‰ (Bindeman, 2008; Eiler et al., 1998, 2000; Garlick, 1966; Gautason and Muehlenbachs, 1998; Harmon and Hoefs, 1995; Hartley et al., 2013; Mattey et al., 1994; Muehlenbachs, 1998; Muehlenbachs and Clayton, 1972; Taylor, 1968; Taylor and Epstein, 1962). In contrast, a much wider range of $\delta^{18}O$ values is observed in seafloor-altered basalt and gabbroic rocks (i.e., 3.6 to +12.7‰, Alt et al., 1986; Kawahata et al., 1987), metasedimentary rocks (3.6 to +12.7‰, Alt et al., 1986), and carbonate and pelagic rocks (+20 to +25‰, Hoefs, 2009; Kolodny and Epstein, 1976; Hoefs, 2009). This wide range of $\delta^{18}O$ values is interpreted as the interaction of surface waters in the Earth's rock cycle (Clayton and Mayeda, 1996). For example, the hydrothermal alteration of oceanic rocks through seawater interaction is an important mechanism for introducing ^{18}O-enriched materials into the mantle during the subduction process (Eiler et al., 1998). Oxygen isotope compositions of eclogites from various metamorphic terranes show that the $\delta^{18}O_{wr}$ values are typically either similar to or greater than the mantle values (e.g., Agrinier et al., 1985; Barnicoat and Cartwright, 1997; Jacob, 2004; Wyck et al., 1996; Fig. 9). However, there are several localities where the UHP eclogites have $\delta^{18}O_{wr}$ values significantly lower than the typical mantle range (e.g., Dabie–Sulu in China with negative values as low as −11‰; Fu et al., 2013; Yui et al., 1997; Zheng et al., 2003a, 2003b; Kokchetav in Kazakhstan with values as low as −4.2‰; Masago et al., 2003). These negative $\delta^{18}O_{wr}$ values have been attributed to ancient meteoric water–rock interactions prior to subduction and resulting UHP metamorphism (Masago et al., 2003; Yui et al., 1995; Zheng et al., 2003c and references therein). In the Sulu region, the lowest reported $\delta^{18}O$ values have been interpreted as reflecting the "Snowball Earth" global glacial event that occurred during the Neoproterozoic ca. 720–635 Ma (Rumble and Yui, 1998; Rumble et al., 2002; Yui et al., 1995, 1997; Zheng et al., 1998, 2002, 2003b). However, the "Snowball Earth" hypothesis in the Neoproterozoic has recently been disputed because negative $\delta^{18}O$ values were discovered for rocks representing >740 Ma and across a much wider area in the Tongbai–Dabie–Sulu Neoproterozoic igneous province in eastern China (e.g., Chen et al., 2011; Fu et al., 2013; Wang et al., 2011). The samples analyzed in our

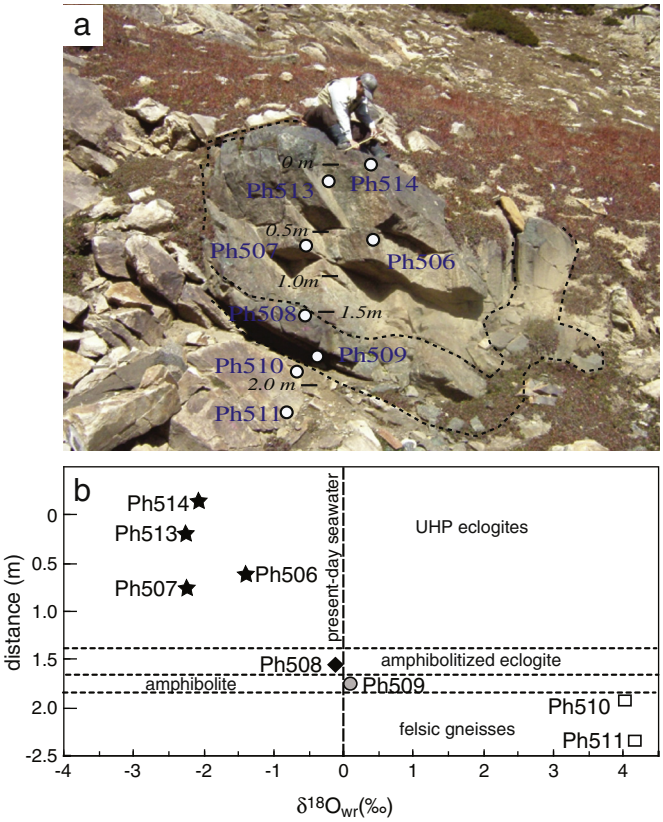

Fig. 6. (a) View of the single UHP eclogite outcrop showing the zoned texture with unaltered and homogeneous core (granular) which progressively grades into amphibolitized parts (fine-grained) toward outer margin. (b) Variation in the $\delta^{18}O$ values with distance (m) across the body. The core of eclogite body (zone between sample Ph507 and Ph514) yielded the lowest $\delta^{18}O$ values, which indicated the least modified by retrogression. Sample Ph506 is located at the interior but yielded higher $\delta^{18}O$ values relative to nearby samples. This possibly resulted from a higher degree of retrogression as evidenced by the higher modal abundance of Zo in this sample. The $\delta^{18}O$ values in samples Ph508 and Ph509 display gradual increase with distance from the center of the eclogite body.

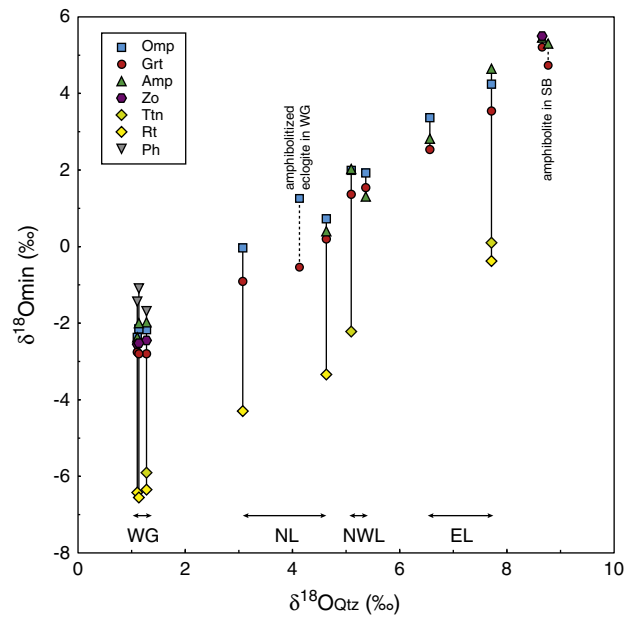

Fig. 7. Plot of $\delta^{18}O_{Qz}$ versus $\delta^{18}O_{min}$ for the analyzed mineral separates. The tie line connects coexisting minerals in the same sample (solid line: eclogites, broken line: amphibolites or amphibolitized eclogite). Double-sided arrows show the range of $\delta^{18}O_{Qz}$ in eclogites for each location. The abbreviations used in the figure are SB: south of Besal, EL: east of Lulusar, NWL: northwest of Lulusar, NL: north of Lulusar, and WG: west of Gittidas.

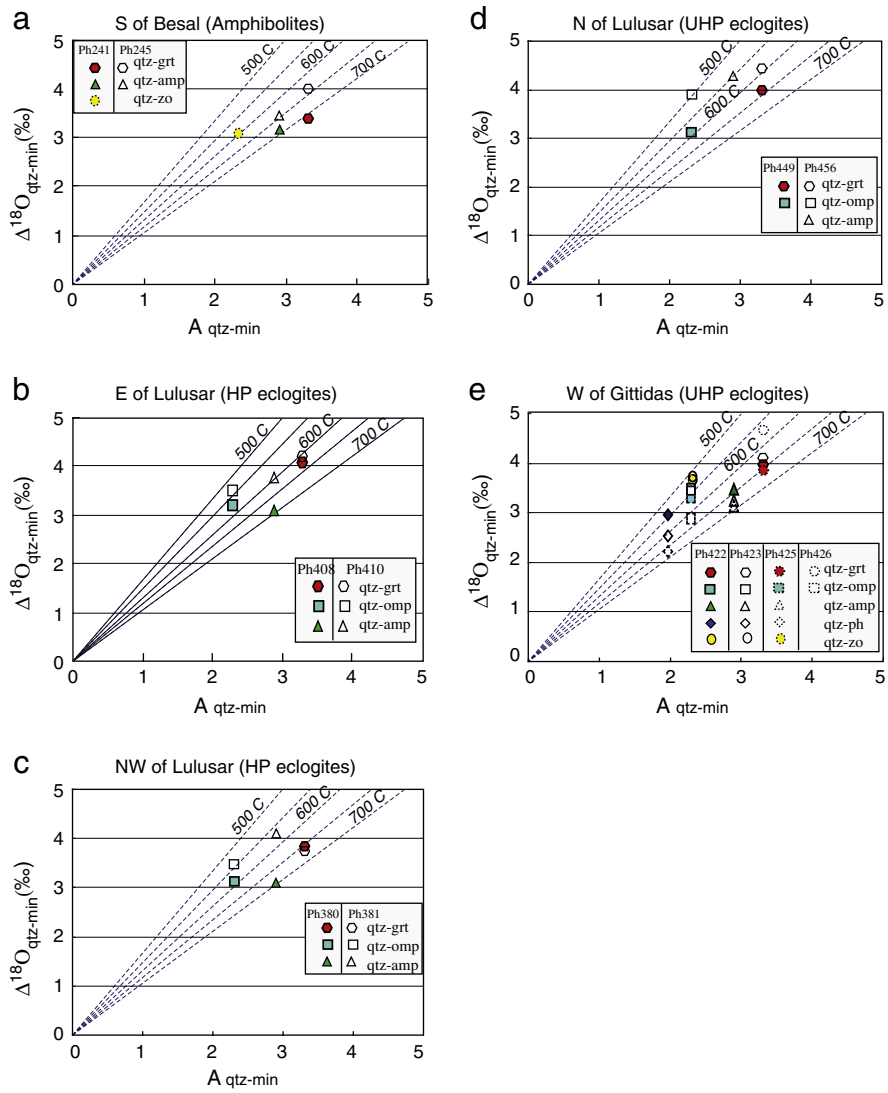

Fig. 8. Isothermal plots for oxygen isotope fractionations between various Qz–mineral pairs over a range of temperatures. Parameter A_{Qz-Min} refers to temperature coefficients in oxygen isotope fractionation equations for quartz-mineral pairs in the form of $10^3 \ln\alpha = A \times 10^6/T^2$ (from Zheng et al., 2003c) and the y-axis is the measured fractionation between Qz and other minerals measured in this study.

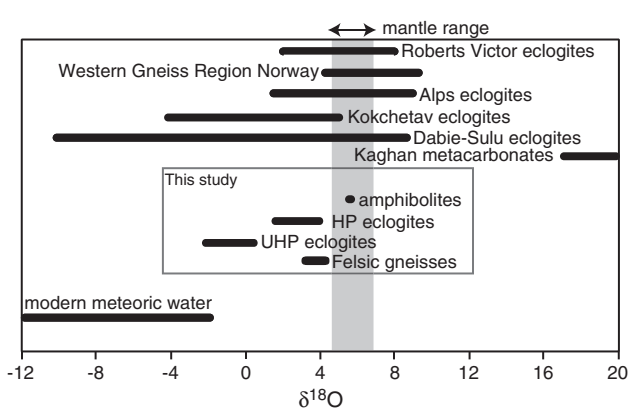

Fig. 9. The $\delta^{18}O$ variations in the Himalayan rocks relative to the eclogites from various terrenes of the world (e.g., Roberts Victor: +2 to +8‰; Jacob, 2004; Western Gneiss Region: +4.3 to +9.5‰, Agrinier et al., 1985; Holsnøy: 6.1 to 7.2‰; Wyck et al., 1996; Western Alps: 4.8 ± 0.9‰, Barnicoat and Cartwright, 1997; Kokchetav: −4.2 to +5.1‰; Masago et al., 2003; and Dabie–Sulu: +8 t −11‰; Yui et al., 1995, 1997; Rumble and Yui, 1998; Zheng et al., 1998, 2002, 2003b; Fu et al., 2013).

study show a range of $\delta^{18}O_{wr}$ values (−2.25‰ to +5.91‰) equal to or lower than the typical mantle values (Fig. 9). These lowered, even negative, $\delta^{18}O$ values require explanation and the most likely scenario for leading to such shifts involves interaction of rocks over a range of temperatures with meteoric water, glacial meltwater or low $\delta^{18}O$ seawater. The negative $\delta^{18}O_{wr}$ values in the Himalayan UHP eclogites and the two distinct trends, (1) a step-wise increase in $\delta^{18}O$ values from UHP eclogites to HP eclogites to amphibolites (regional scale) and (2) progressively increasing $\delta^{18}O$ values from eclogites to amphibolites on local scale (single outcrop), suggest that either the rocks formed from a low $\delta^{18}O$ source or they acquired negative $\delta^{18}O$ values after emplacement. If we assume that the rocks had a low $\delta^{18}O$ source then do all of the analyzed samples not have similar values, given their similar protoliths? Also, when and by what process was $\delta^{18}O_{wr}$ systematically increased? The discussion below provides a plausible explanation.

7.1. ^{18}O-depleted magma source

The magma source for the Permian Panjal Traps (protolith of the Kaghan Valley eclogites) could perhaps have been ^{18}O-depleted. However, the low $\delta^{18}O$ values in the felsic gneisses (this study) and metacarbonates (Spencer, 1993) argue against the argument of the

^{18}O-depleted magma source to explain the low δ^{18}O eclogites and point to a different scenario. There are several examples of basaltic rocks with possible ^{18}O-depleted magma sources, including the Icelandic basalts (Hattori and Muehlenbachs, 1982), Yellowstone volcanics (Bindeman and Valley, 2001; Bindeman et al., 2008), eastern China UHP rocks (Fu et al., 2013; Rumble et al., 2002; Wei et al., 2008; Zheng et al., 1998) and mafic dykes of the Koegel Fontein Complex, South Africa (Curtis et al., 2013). Iceland is a high latitude example where basaltic rocks have δ^{18}O values as low as −10‰ (Hattori and Muehlenbachs, 1982). Hartley et al. (2013) concluded that the negative δ^{18}O values in Icelandic basalts resulted from the hydrothermal alteration of the rocks due to the percolation of surface waters that originated from ^{18}O-depleted precipitation. In contrast, mafic dykes of the Koegel Fontein Complex yielding low or negative δ^{18}O values (down to −2‰) were attributed to an ^{18}O-depleted magma source in which the low δ^{18}O values resulted from the meteoric water–rock interaction during Pan-African (i.e. when South Africa was at southern high latitudes) rifting (Curtis et al., 2013). Bindeman and Valley (2001) and Bindeman et al. (2008) proposed partial melting of hydrothermally altered material from an earlier stage of volcanism for the low or negative δ^{18}O magma source for some of these locations. For eastern China rocks, a possible reason for the low or negative δ^{18}O values is the assimilation of crust with low δ^{18}O (e.g. Fu et al., 2013; Rumble et al., 2002; Wang et al., 2011; Zheng et al., 1998). We propose a scenario in which meteoric water–rock interaction lowered δ^{18}O values of not only eclogites, but also the surrounding felsic gneisses and metacarbonates, the alteration of the latter two rock types arguing against the derivation of the low δ^{18}O of the basalts by inheritance from their magmatic source.

7.2. Hydrothermal alteration of the protolith

It is most likely that the protolith rocks (Permian Panjal Trap magmatism) of the Himalayan eclogites were hydrothermally altered after their emplacement. Paleomagnetic data and stratigraphic evidence suggest that the Indian plate was in contact with Africa, Australia and Antarctica (Gondwana continent) until the Cretaceous period (Acton, 1999; Klootwijk et al., 1992). During the Permian, India was located at southern high latitudes of ~60°S (Scotese, 1984) for the time period when the protoliths of the eclogites formed (U–Pb zircon protolith age; Rehman et al., 2013). Because of their position at high latitude, and the related cold climate, the rocks could have interacted with low δ^{18}O meteoric water during hydrothermal alteration at high temperature conditions at shallow levels. Glacial ice caps and cold environments have been reported for the Permo-Triassic period on the Indian plate (Scotese, 1984; Scotese Paleomap Project: http://www.scotese.com/earth.htm) and were confirmed through study of brachiopods recovered from the Permian sedimentary deposits of Sydney and Tasmania, the latter which were located in the east but at similar southern latitudes (Mii et al., 2012). In addition, the presence of glacial tillites in Australia and Siberia indicates a drop in sea levels during and/or at the end of the Permian (Mii et al., 2012), producing glaciers in the southern polar areas in Gondwana potentially provided a source for ^{18}O-depleted waters. These lines of evidence strongly support our interpretation of the unusual δ^{18}O values in the eclogites. Moreover, the presence of tuffaceous material (Honegger et al., 1982; Shellnutt et al., 2012 and references therein) and the absence of pillow lavas in the Panjal Traps indicate subaerial conditions. If the climate was cold, it is likely that the water/ice–rock interaction with the protolith rocks would have lowered the rock δ^{18}O values. The rocks overlying and in contact with these eclogites are felsic gneisses which also have low δ^{18}O values (ca. +3.03 to +4.58‰), lower than those commonly found in most sedimentary rocks (e.g., +12 to +20‰; Hoefs, 2009; Kolodny and Epstein, 1976). These lower values in felsic gneisses further support our notion that the low δ^{18}O values is a regional tendency which does not depend on the type of protolith. The δ^{18}O of the altered basalt also depends on water/rock ratio during hydrothermal alternation. The degree of alteration which depends on different water/rock ratios, however, is heterogeneous even on the metric scale (Rumble and Yui, 1998; Zheng et al., 1998). If the degree of alteration of the protolith was significantly high and different in various eclogite blocks, this could be reflected through other geochemical tracers as well (e.g., major and trace elements) which is not. The chemical composition of whole-rock (regardless of different sampling points) shows that most of the eclogites and amphibolitized eclogites have more or less identical chemistry with minor local variations except two samples (Ph380 and Ph381 which have slightly higher Fe–Ti, REE and HFS element contents; see Table 2 in Rehman et al., 2008). Thus, it is unlikely that the regional-scale low δ^{18}O tendency was attributed to the high water/rock ratio in low to middle latitude. Seawater–rock interaction could be an alternate source for the low δ^{18}O values in the Himalayan metabasites. The δ^{18}O value of seawater is one of the most controversial issues in paleoceanography (e.g. Veizer et al., 1999). According to the current knowledge, it is estimated as the δ^{18}O values of Permian seawater should be between 0 and −5‰ (Ivany and Runnegar, 2010; Veizer et al., 1999). Even if the δ^{18}O values of paleoseawater is estimated to be −5‰, the δ^{18}O of the hydrothermally altered basalt caused by the interaction with seawater-derived fluid can change down to ~0‰ at least (Kawahata et al., 1987).

In contrast, the progressive increase in δ^{18}O values from UHP eclogites toward amphibolites indicates the effects of late-stage retrogression. If the mafic rocks were subducted to mantle depth (UHP stage) within a relatively closed system (with little or no hydration or influx from crustal rocks at such greater depths), they could have

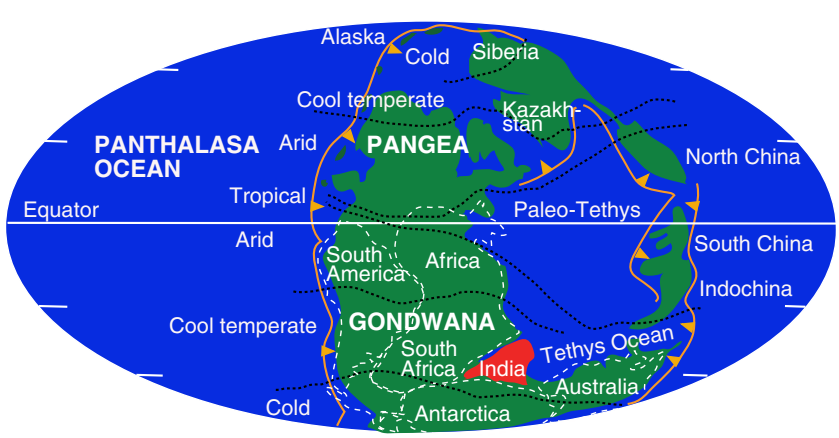

Fig. 10. Paleo-reconstructed map of continents in Permian indicating southern high latitudes for the Indian plate (redrawn from Scotese Paleomap Project: http://www.scotese.com/earth.htm).

retained their protolithic low $\delta^{18}O$ acquired by surface/near-surface hydrothermal alteration. These low $\delta^{18}O$ values could have been largely unmodified by prograde metamorphism, the latter which is generally unable to lower $\delta^{18}O$ values by more than 1 to 2‰ (Polyakov and Kharlashina, 1994; Valley, 1986, 2003). However, in contrast, during the exhumation-related retrogression, involving externally derived metamorphic fluids, at low temperatures, could have been capable of producing increase in the $\delta^{18}O$ values. The rocks that experienced UHP metamorphism but smaller degrees of retrogression retained the lowest $\delta^{18}O_{wr}$ values and the rocks exposed to a higher degree of retrogression (amphibolitized eclogites ➔ amphibolites) have progressively higher $\delta^{18}O_{wr}$. The $\delta^{18}O$ values of meteoric water in Iceland (a modern high-latitude volcanic environment in which basaltic rocks are subaerially altered) are consistently low (−13 to −10‰), as are the hydrothermally altered rocks (−7.7 ± 2.4‰) through which they percolate (Hattori and Muehlenbachs, 1982). Importantly, the high latitude of Iceland (~60°N) and its cold climate control its oxygen isotope distribution. The paleo-plate reconstructions, based on the models of Scotese (1984), place the Indian plate at the time of Panjal Trap volcanism at southern high latitudes (~60°S; Fig. 10). This geographic location provides ideal conditions for the availability of meteoric waters with highly negative $\delta^{18}O$ to hydrothermally alter the Panjal Trap basalts and nearby rocks.

7.3. Effect of prograde metamorphism

Prograde metamorphism and dehydration reactions could have depleted the $\delta^{18}O$ values in the Himalayan metabasites. However, it is unlikely that this depletion significantly changes the oxygen isotope compositions of the rocks because the effects of dehydration on $\delta^{18}O$ are small (<1‰; Valley, 1986). An influx of fluid from the surrounding felsic gneisses and metacarbonates, at or near peak metamorphic P–T, would have led to increase in the $\delta^{18}O$ values in the metabasites. However, the metabasites best preserving peak metamorphic mineral assemblages tend not to be shifted to higher $\delta^{18}O$ values relative to mantle values (>+5.7‰) and in fact have considerably lower $\delta^{18}O$. Thus, we believe that the strongly negative $\delta^{18}O_{wr}$ values of the Kaghan rocks, and the normal enrichment pattern of ^{18}O in the minerals that are stable at the eclogite facies stage, indicate ^{18}O-depletion that occurred prior to subduction and was preserved during prograde metamorphism.

7.4. Resetting of the $\delta^{18}O$ by late-stage retrogression

The $\delta^{18}O$ values in metamorphic rocks can increase relative to their magmatic protoliths and high P–T grade counterparts during cooling and/or retrograde metamorphism (Muehlenbachs, 1998). However, increases or decreases in the $\delta^{18}O$ values depend on the source of the hydrothermal fluids during retrogression. The $\delta^{18}O_{wr}$ values in the Kaghan Valley metabasites are lower in high-grade rocks and increase step-wise with increasing retrogression. These findings suggest greater interaction of these retrogressed rocks during cooling with ^{18}O-rich fluids that were available during retrogression. A similar pattern of increasing $\delta^{18}O$ values was observed on a local scale within a single UHP eclogite body. Lower or negative $\delta^{18}O_{wr}$ values were preserved in the core of the eclogite body (unaltered central part) and progressively increased toward its outer margin. Thus, exhumation-related retrogression directly influenced the $\delta^{18}O$ values. A higher degree of retrogression and a higher rate of external fluid interaction with the rocks potentially resulted in the trend of increase in $\delta^{18}O$. These findings imply that the lower $\delta^{18}O$ values were produced in the protolith rocks before their subduction. As these rocks were returning to the surface, isotopic exchange with the surrounding metasedimentary rocks, presumably via metamorphic fluids, resulted in higher $\delta^{18}O$ values. We conclude that the protoliths of the Himalayan eclogites were hydrothermally altered by meteoric water, then metamorphosed to UHP conditions largely as closed system. Some of the eclogites (least retrogressed) retained their oxygen isotope compositions during both subduction and exhumation, whereas, other eclogites (slightly to highly amphibolitized) were altered by the infiltration of ^{18}O-rich fluids from the surrounding felsic and hydrous low-grade rocks. These results are consistent with the petrographic observations recorded in the Nepal Himalayas during late-stage retrogression (Kaneko, 1997). Similarly, fluid-infiltration from hydrous low-grade rocks into anhydrous high-grade UHP–HP rocks was observed in Kokchetav area by Terabayashi et al. (2002) and Masago et al. (2010).

Acknowledgment

This work was carried out under the Visiting Researcher's Program of the ISEI, Okayama University and was partially supported by the Kagoshima University's Young Researchers Visiting Program to Potsdam University, Germany. We are thankful for the critical and constructive review by Gray Bebout and an anonymous reviewer which improved the manuscript and for the editorial handling by Sun-Lin Chung.

References

Acton, G.D., 1999. Apparent Polar Wander of India since the Cretaceous with Implications for Regional Tectonics and True Polar Wander, in the Indian Subcontinent and Gondwana: A Paleomagnetic and Rock Magnetic Perspective. In: Radhakrishna, T., Piper, J.D.A. (Eds.), Memoir Geological Society of India 44, pp. 129–175.

Agrinier, P., Javoy, M., Smith, D.C., Pineau, F., 1985. Carbon and oxygen isotopes in eclogites, amphibolites, veins and marbles from the Western Gneiss Region, Norway. Chemical Geology 52, 145–162.

Alt, J.C., Muehlenbachs, K., Honnorez, J., 1986. An oxygen isotopic profile through the upper kilometer of the oceanic crust, DSDP Hole 504B. Earth and Planetary Science Letters 80, 217–229.

Barnicoat, A.C., Cartwright, I., 1997. The gabbro–eclogite transformation: an oxygen isotope and petrographic study of west Alpine ophiolites. Journal of Metamorphic Geology 15, 93–104.

Bindeman, I.N., 2008. Oxygen isotopes in mantle and crustal magmas as revealed by single crystal analysis. Reviews in Mineralogy and Geochemistry 69, 445–478.

Bindeman, I.N., Valley, J.W., 2001. Low-$\delta^{18}O$ rhyolites from Yellowstone: magmatic evolution based on analyses of zircons and individual phenocrysts. Journal of Petrology 42, 1491–1517.

Bindeman, I.N., Fu, B., Kita, N., Valley, J.W., 2008. Origin and evolution of silicic magmatism at Yellowstone based on ion microprobe analysis of isotopically zoned zircons. Journal of Petrology 49, 163–193.

Chacko, T., Hu, X., Mayeda, T.K., Clayton, R.N., Goldsmith, J.R., 1996. Oxygen isotope fractionations in muscovite, phlogopite, and rutile. Geochimica et Cosmochimica Acta 60, 2595–2608.

Chamberlain, C.P., Zeitler, P.K., Erickson, E., 1991. Constraints on the tectonic evolution of the northwestern Himalaya from geochronologic and petrologic studies of the Babusar Pass, Pakistan. Journal of Geology 99, 829–849.

Chaudhry, M.N., Ghazanfar, M., 1987. Geology, structure and geomorphology of upper Kaghan Valley, Northwestern Himalaya, Pakistan. Geological Bulletin University of Punjab 22, 13–57.

Chen, Y.X., Zheng, Y.F., Chen, R.X., Zhang, S.B., Li, Q.L., Dai, M.N., Chen, L., 2011. Metamorphic growth and recrystallization of zircons in extremely ^{18}O-depleted rocks during eclogite-facies metamorphism: evidence from U–Pb ages, trace elements, and O–Hf isotopes. Geochimica et Cosmochimica Acta 75, 4877–4898.

Clayton, R.N., Mayeda, T.K., 1996. Oxygen isotope studies of achondrites. Geochimica et Cosmochimica Acta 60, 1999–2017.

Curtis, C.G., Harris, C., Trumbull, R.B., Beer, C., Mudzanani, L., 2013. Oxygen isotope diversity in the anorogenic Koegel Fontein Complex of South Africa: a case for basement control and selective melting for the production of low $\delta^{18}O$ magmas. Journal of Petrology 54, 1259–1283.

Eiler, J.M., 2001. Oxygen isotope variations of basaltic lavas and upper mantle rocks. In: Valley, J.W., Cole, D.R. (Eds.), Stable Isotope Geochemistry. Stable Isotope, Reviews in Mineralogy and Geochemistry 43, pp. 319–364.

Eiler, J.M., McInnes, B., Valley, J.W., Graham, C.M., Stolper, E.M., 1998. Oxygen isotope evidence for slab-derived fluids in the sub-arc mantle. Nature 393, 777–781.

Eiler, J.M., Schiano, P., Kitchen, N., Stolper, E.M., 2000. Oxygen-isotope evidence for recycled crust in the sources of mid-ocean ridge basalts. Nature 403, 530–534.

Fu, B., Kita, N., Wilde, S.A., Liu, X., Cliff, J., Greig, A., 2013. Origin of the Tongbai–Dabie–Sulu Neoproterozoic low-$\delta^{18}O$ igneous province, east-central China. Contributions to Mineralogy and Petrology 165, 641–662.

Garlick, G.D., 1966. Oxygen isotope fractionation in igneous rocks. Earth and Planetary Science Letters 1, 361–368.

Gautason, B., Muehlenbachs, K., 1998. Oxygen isotope fluxes associated with high-temperature processes in the rift zones of Iceland. Chemical Geology 145, 275–286.

Greco, A., Martinotti, G., Papritz, K., Ramsay, J.G., Rey, R., 1989. The Himalayan crystalline rocks of the Kaghan Valley (NE-Pakistan). Eclogae Geologicae Helvetiae 82, 603–627.

Green, T.H., Helman, P.L., 1982. Fe–Mg partitioning between coexisting garnet and phengite at high pressure, and comments on a garnet–phengite geothermometer. Lithos 15, 253–266.

Guillot, S., Garzanti, G., Baratoux, D., Marquer, D., Maheo, G., de Sigoyer, J., 2003. Reconstructing the total shortening history of the NW Himalaya. Geochemistry, Geophysics, Geosystems 4, 1064.

Harmon, R.S., Hoefs, J., 1995. Oxygen isotope heterogeneity of the mantle deduced from global ^{18}O systematics of basalts from different geotectonic settings. Contributions to Mineralogy and Petrology 120, 95–114.

Hartley, M.E., Thordarson, T., Fitton, J.G., EIMF, 2013. Oxygen isotopes in melt inclusions and glasses from the Askja volcanic system, North Iceland. Geochimica et Cosmochimica Acta 123, 55–73.

Hattori, K., Muehlenbachs, K., 1982. Oxygen isotope ratios of the Icelandic crust. Journal of Geophysical Research 87, 6559–6565.

Hoefs, J., 2009. Stable Isotope Geochemistry, 6th ed. Springer-Verlag, Berlin.

Honegger, K., Dietrich, V., Frank, W., Gansser, A., Thöni, M., Trommsdorf, V., 1982. Magmatism and metamorphism in the Ladakh Himalaya (the Indus–Tsangpo suture zone). Earth and Planetary Science Letters 60, 253–292.

Ivany, L.C., Runnegar, B., 2010. Early Permian seasonality from bivalve $\delta^{18}O$ and implications for the oxygen isotopic composition of seawater. Geology 38, 1027–1030.

Jacob, D.E., 2004. Nature and origin of eclogite xenoliths from kimberlites. Lithos 77, 295–316.

Kaneko, Y., 1997. Two-step exhumation model of the Himalayan metamorphic belt, central Nepal. Journal of Geological Society of Japan 103, 203–226.

Kaneko, Y., Katayama, I., Yamamoto, H., Misawa, K., Ishikawa, M., Rehman, H.U., Kausar, A.B., Shiraishi, K., 2003. Timing of Himalayan ultrahigh-pressure metamorphism: sinking rate and subduction angle of the Indian continental crust beneath Asia. Journal of Metamorphic Geology 21, 589–599.

Kawahata, H., Kusakabe, M., Kikuchi, Y., 1987. Strontium, oxygen, and hydrogen isotope geochemistry of hydrothermally altered and weathered rocks in DSDP hole 504B, Costa Rica rift. Earth and Planetary Science Letters 85, 343–355.

Klootwijk, C.T., Gee, J.S., Peirce, J.W., Smith, G.M., McFadden, P.L., 1992. An early India–Asia contact: paleomagnetic constraints from Ninetyeast Ridge, ODP Leg 121. Geology 20, 395–398.

Kolodny, Y., Epstein, S., 1976. Stable isotope geochemistry of deep sea cherts. Geochimica et Cosmochimica Acta 40, 1195–1209.

Kusakabe, M., Maruyama, S., Nakamura, T., Yada, T., 2004. CO_2 laser fluorination technique for analysis of oxygen three isotopes of rocks and minerals. Journal of Mass Spectrometry Society of Japan 52, 205–212.

Lacroix, B., Vennemann, T., 2013. Empirical calibration of the oxygen isotope fractionation between chlorite and quartz. Geophysical Research Abstracts 15 (EGU2013-9158, 2013, EGU General Assembly 2013).

MacGregor, I., Manton, W.I., 1986. Roberts Victor eclogites: ancient oceanic crust. Journal of Geophysical Research 91, 14063–14079.

Masago, H., Rumble, D., Ernst, W.G., Maruyama, S., 2003. A discovery of the very Low $\delta^{18}O$ eclogites from the Kokchetav massif, Northern Kazakhstan. Journal of Metamorphic Geology 21, 579–587.

Masago, H., Omori, S., Maruyama, S., 2010. Significance of retrograde hydration in collisional metamorphism: a case study of water infiltration in the Kokchetav ultrahigh-pressure metamorphic rocks, northern Kazakhstan. Gondwana Research 18, 205–212.

Mattey, D., Lowry, D., MacPherson, C., 1994. Oxygen isotope composition of mantle peridotite. Earth and Planetary Science Letters 128, 231–241.

Mii, H.S., Shi, G.R., Cheng, C.J., Chen, Y.Y., 2012. Permian Gondwanaland paleoenvironment inferred from carbon and oxygen isotope records of brachiopod fossils from Sydney Basin, southeast Australia. Chemical Geology 291, 87–103.

Muehlenbachs, K., 1998. The oxygen isotopic composition of the oceans, sediments and the seafloor. Chemical Geology 145, 263–273.

Muehlenbachs, K., Clayton, R.N., 1972. Oxygen isotope studies of fresh and weathered submarine basalts. Canadian Journal of Earth Sciences 9, 172–184.

O'Brien, P.J., Zotov, N., Law, R., Khan, M.A., Jan, M.Q., 2001. Coesite in Himalayan eclogite and implications for models of India–Asia collision. Geology 29, 435–438.

Ongley, J., Basu, A., Kyser, T.K., 1987. Oxygen isotopes in coexisting garnets, clinopyroxenes and phlogopites of Roberts Victor eclogites: implications for petrogenesis and mantle metasomatism. Earth and Planetary Science Letters 99, 362–379.

Papritz, K., Rey, R., 1989. Evidence for the occurrence of Panjal Trap Basalts in the Lesser and Higher Himalaya of the Western Syntaxis area, NE Pakistan. Eclogae Geologicae Helvetiae 82, 603–627.

Parrish, R.R., Gough, S.J., Searle, M.P., Waters, D.J., 2006. Plate velocity exhumation of ultrahigh-pressure eclogites in the Pakistan Himalaya. Geology 34, 989–992.

Perkins, G.B., Sharp, Z.D., Selverstone, J., 2006. Oxygen isotope evidence for subduction and rift-related mantle metasomatism beneath the Colorado Plateau–Rio Grande rift transition. Contributions to Mineralogy and Petrology 151, 633–650.

Polyakov, V.B., Kharlashina, N.N., 1994. Effect of pressure on equilibrium isotopic fractionation. Geochimica et Cosmochimica Acta 58, 4739–4750.

Powell, R., 1985. Regression diagnostic and robust regression in geothermometer/geobarometer calibration: the garnet–clinopyroxene geothermometer revisited. Journal of Metamorphic Geology 3, 231–243.

Rehman, H.U., Yamamoto, H., Kaneko, Y., Kausar, A.B., Murata, M., Ozawa, H., 2007. Thermobaric structure of the Himalayan Metamorphic Belt in Kaghan Valley, Pakistan. Journal of Asian Earth Sciences 29, 390–406.

Rehman, H.U., Yamamoto, H., Nakamura, E., Khalil, M.A., Zafar, M., Khan, T., 2008. Metamorphic history and tectonic evolution of the Himalayan UHP eclogites in Kaghan valley, Pakistan. Journal of Mineralogical and Petrological Sciences 103, 242–254.

Rehman, H.U., Kobayashi, K., Tsujimori, T., Ota, T., Nakamura, E., Yamamoto, H., Kaneko, Y., Khan, T., 2012. Sm–Nd and Lu–Hf isotope geochemistry of the Himalayan high- and ultrahigh-pressure eclogites, Kaghan Valley, Pakistan. In: Panagiotaras, D. (Ed.), Geochemistry-Earth's System Processes Inteck. Rijeka, Croatia, pp. 105–126.

Rehman, H.U., Kobayashi, K., Tsujimori, T., Ota, T., Yamamoto, H., Nakamura, E., Kaneko, Y., Khan, T., Terabayashi, M., Yoshida, K., Hirajima, T., 2013. Ion microprobe U–Th–Pb geochronology and study of micro-inclusions in zircon from the Himalayan high- and ultrahigh-pressure eclogites, Kaghan Valley of Pakistan. Journal of Asian Earth Sciences 63, 179–196.

Rumble, D., Yui, T.F., 1998. The Qinglongshan oxygen and hydrogen isotope anomaly near Donghai in Jiangsu Province, China. Geochimica et Cosmochimica Acta 62, 3307–3321.

Rumble, D., Giorgis, D., Ireland, T., Zhang, Z., Xu, H., Yui, T.F., Yang, J., Xu, Z., 2002. Low $\delta^{18}O$ zircons, U–Pb dating, and the age of the Qinglongshan oxygen and hydrogen isotope anomaly near Donghai in Jiangsu Province, China. Geochimica et Cosmochimica Acta 66, 2299–2306.

Scotese, C.R., 1984. An introduction to this volume: Paleozoic paleomagnetism and the assembly of Pangaea. In: Van der Voo, R., Scotese, C.R., Bonhommet, N. (Eds.), Plate Reconstruction from Paleozoic Paleomagnetism. AGU Geodynamic Series vol. 12, pp. 1–10 (Washington D.C.).

Searle, M.P., Khan, M.A., Fraser, J.E., Gough, S.J., Jan, M.Q., 1999. The tectonic evolution of the Kohistan collision belt along the Karakoram Highway transect, north Pakistan. Tectonics 18, 929–949.

Shellnutt, J.G., Bhat, G.M., Wang, K.L., Brookfield, M.E., Dostal, J., Jahn, B.M., 2012. Origin of the silicic volcanic rocks of the Early Permian Panjal Traps, Kashmir, India. Chemical Geology 334, 154–170.

Spencer, D.A., 1993. Tectonics of the Higher and Tethyan Himalaya, Pakistan: Implications of an Early Collisional, High-Pressure (Eclogite Facies) Metamorphism to the Himalayan Belt(Ph. D thesis) Eidgenossaische Technische, Zurich.

Spencer, D.A., Gebauer, D., 1996. SHRIMP Evidence for a Permian Protolith Age and a 44 Ma Metamorphic Age for the Himalayan Eclogites (Upper Kaghan, Pakistan): Implication for the Subduction of the Tethys and the Subdivision Terminology of the NW Himalaya: Himalayan–Karakoram–Tibet Workshop, 11th, (Flagstaff, Arizona, USA), Abstract Volume. pp. 147–150.

Tahirkheli, R.A.K., Mattauer, M., Proust, F., Tapponnier, P., 1979. The India Eurasia suture zone in northern Pakistan: synthesis and interpretation of recent data at plate scale. In: Farah, A., DeJong, K.A. (Eds.), Geodynamics of Pakistan. Geological Survey of Pakistan, pp. 125–130.

Tanaka, R., Nakamura, E., 2013. Determination of ^{17}O-excess of terrestrial silicate/oxide minerals with respect to Vienna Standard Mean Ocean Water (VSMOW). Rapid Communications in Mass Spectroscopy 27, 285–297.

Taylor Jr., H.P., 1968. The oxygen isotope geochemistry of igneous rocks. Contributions to Mineralogy and Petrology 19, 1–71.

Taylor Jr., H.P., Epstein, S., 1962. Relationship between $^{18}O/^{16}O$ ratios in coexisting minerals of igneous and metamorphic rocks. Geological Society of America Bulletin 73, 675–694.

Terabayashi, M., Ota, T., Yamamoto, H., Kaneko, Y., 2002. Contact metamorphism of the Daulet Suite by solid-state emplacement of the Kokchetav UHP–HP metamorphic slab. International Geology Review 44, 819–830.

Valley, J.W., 1986. Stable isotope geochemistry of metamorphic rocks. In: Valley, J.W., Taylor Jr., H.P., O'Neil, J.R. (Eds.), Stable Isotopes in High Temperature Geological Processes. Reviews in Mineralogy 16, pp. 445–489.

Valley, J.W., 2003. Oxygen isotopes in zircon. In: Hanchar, J., Hoskin, P. (Eds.), Zircon. Reviews in Mineralogy and Geochemistry 53, pp. 343–380.

Veizer, J., Ala, D., Azmy, K., Bruckschen, P., Buhl, D., Bruhn, F., Carden, G.A.F., Diener, A., Ebneth, S., Godderis, Y., Jasper, T., Korte, C., Pawellek, F., Podlaha, O.G., Strauss, H., 1999. $^{87}Sr/^{86}Sr$, $\delta^{13}C$ and $\delta^{18}O$ evolution of Phanerozoic seawater. Chemical Geology 161, 59–88.

Wang, X.C., Li, Z.X., Li, X.H., Li, Q.L., Tang, G.Q., Zhang, Q.R., Liu, Y., 2011. Nonglacial origin for low-$\delta^{18}O$ Neoproterozoic magmas in the South China Block: evidence from new in-situ oxygen isotope analysis using SIMS. Geology 39, 735–738.

Waters, D.J., Martin, H.N., 1993. Geobarometry in phengite-bearing eclogites. Terra Abstracts 5, 410–411.

Wei, C.S., Zhao, Z.F., Spicuzza, M.J., 2008. Zircon oxygen isotopic constraint on the sources of late Mesozoic A-type granites in eastern China. Chemical Geology 250, 1–15.

Whitney, D.L., Evans, B.W., 2010. Abbreviations for names of rock-forming minerals. American Mineralogist 95, 185–187.

Wilke, F.D.H., O'Brien, P.J., Gerdes, A., Timmerman, M.J., Sudo, M., Khan, M.A., 2010a. The multistage exhumation history of the Kaghan Valley UHP series, NW Himalaya, Pakistan from U–Pb and $^{40}Ar/^{39}Ar$ ages. European Journal of Mineralogy 22, 703–719.

Wilke, F.D.H., O'Brien, P.J., Altenberger, U., Konrad-Schmolke, M., Khan, M.A., 2010b. Multi-stage reaction history in different eclogite types from the Pakistan Himalaya and implications for exhumation processes. Lithos 114, 70–85.

Wyck, N.V., Valley, J.W., Austrheim, H., 1996. Oxygen and carbon isotopic constraints on the development of eclogites, Holsnøy, Norway. Lithos 38, 129–145.

Yui, T.F., Rumble, D., Lo, C.H., 1995. Unusually low delta ^{18}O ultra-high-pressure metamorphic rocks from the Sulu Terrain, eastern China. Geochimica et Cosmochimica Acta 59, 2859–2864.

Yui, T.F., Rumble, D., Chen, C.H., Lo, C.H., 1997. Stable isotope characteristics of eclogites from the ultra-high-pressure metamorphic terrain, east-central China. Chemical Geology 137, 135–147.

Zheng, Y.F., 1999. Oxygen isotope fractionation in carbonate and sulfate minerals. Geochemical Journal 33, 109–126.

Zheng, Y.F., Fu, B., Li, Y., Xiao, Y., Li, S., 1998. Oxygen and hydrogen isotope geochemistry of ultrahigh-pressure eclogites from the Dabie Mountains and the Sulu terrane. Earth and Planetary Science Letters 155, 113–129.

Zheng, Y.F., Wang, Z.R., Li, S.G., Zhao, Z.F., 2002. Oxygen isotope equilibrium between eclogite minerals and its constraints on mineral Sm–Nd chronometer. Geochimica et Cosmochimica Acta 66, 625–634.

Zheng, Y.F., Fu, B., Gong, B., Li, L., 2003a. Stable isotope geochemistry of ultrahigh pressure metamorphic rocks from the Dabie–Sulu orogeny in China: implications for geodynamics and fluid regime. Earth Science Reviews 62, 105–161.

Zheng, Y.F., Zheng, R.W., Li, S.G., Zhao, Z.F., 2003b. Oxygen isotope equilibrium between eclogite minerals and its constraints on mineral Sm–Nd chronometer. Geochimica et Cosmochimica Acta 66, 625–634.

Zheng, Y.F., Zhao, Z.F., Li, S.G., Gong, B., 2003c. Oxygen isotope equilibrium between ultrahigh-pressure metamorphic minerals and its constraints on Sm–Nd and Rb–Sr chronometers, in geochronology: linking the isotopic record with petrology and textures. Geological Society of London, Special Publication 220, 93–117.